Variation of molecular ions in the inner magnetosphere observed by the Arase satellite

A. Nagatani[1], Y. Miyoshi[1], K. Asamura[2], L. M. Kistler[1,3], S. Nakamura[1], K. Seki[4], Y. Ogawa[5] , and I. Shinohara[2]

[1] Institute for Space-Earth Environmental Research, Nagoya University, Nagoya, Japan

[2] JAXA, Sagamihara, Japan

[3] University of New Hampshire, Durham, NH, US.

[4] University of Tokyo, Tokyo, Japan

[5] National Institute for Polar Research, Tachikawa, Japan

Corresponding author: Yoshizumi Miyoshi (miyoshi@isee.nagoya-u.ac.jp)

Key Points:

- Systematic molecular ion observations in the inner magnetosphere for 6.5 years.
- Molecular ion counts increase following enhancements in the solar wind dynamic pressure.
- The ratio of molecular ions to O^+ was lower in the rising phase of the solar cycle than that during the solar minimum.

Abstract

We analyzed time-of-flight (TOF) data from the Arase satellite to investigate temporal variations of O_2^+, NO^+, and N_2^+ at 19.2 keV/q in the inner magnetosphere for 6.5 years from the solar declining to rising phases. Molecular ion counts were estimated by subtracting the background contamination of oxygen counts. While the number of clear molecular events was small, the estimated molecular ion counts exhibited good correlation with the solar wind dynamic pressure and SYM-H index. Long-term variations of molecular ions were different from that of oxygen ions. Additionally, we discuss the importance of the solar wind dynamic pressure in causing the escape of molecular ions into the magnetosphere through an increase in the convection electric field, which causes different evolutions of oxygen ions and molecular ions.

Plain language summary

Molecular ions (O_2^+, NO^+, and N_2^+) have been observed in the magnetosphere. Molecular ions in the ionosphere are required to obtain energy through short-lived reactions with electrons to escape from low altitudes at the ionosphere to the magnetosphere. The escaping mechanisms of molecular ions are not fully understood. This study analyzed 6.5 years of data from the Arase satellite to investigate long-term variations of molecular ions in the inner magnetosphere. We developed a reliable dataset of the molecular ions from the TOF observations. Our results suggest solar wind dynamic pressure increases can enhance molecular ions escape from the ionosphere into the magnetosphere through the increase of the convection electric fields.

1 Introduction

[1]

Heavy ions with single charge states, such as O^+ and N^+, and molecular ions such as O_2^+, NO^+, and N_2^+, originate from the Earth's ionosphere, and are transported to the magnetosphere. The outflow of O+ ions has been the subject of numerous studies (e.g., Yau et al., 2007; Glocer et al., 2012; Keika et al., 2013; Ilie et al., 2015), and escape mechanisms that involve photoionization, electron precipitation, ion-electron-neutral chemistry, and collisions, have been considered. Compared to atomic ions, molecular ions peak at much lower altitudes, ~150-200 km, and therefore are required to obtain energy in short dissociative recombination lifetimes with electrons to escape from low altitudes; however, the molecular ion outflow mechanisms are not well known (Lin and Ilie, 2022).

[2]

Molecular ions in the magnetosphere were first reported using the DE-1 satellite (Craven et al., 1985). The DE-1 satellite observations suggest that molecular ions are produced in the polar cusp region, and transported to the nightside and polar cap by convection electric fields. The Polar satellite observed molecular ions and found that their detection was more sensitive to enhanced geomagnetic conditions than that for O^+ detection (Lennartsson et al., 2000). They suggested that the pathway and energization mechanisms of molecular ions are distinct from those of O^+, because molecular ions appear to be more enhanced during geomagnetic activity. Recently, Takada et al. (2021) investigated the upflows of molecular ions in the thermosphere using EISCAT radar observations, and showed a significant outflow of molecular ions during coronal mass ejection (CME)- and corotating interaction region (CIR) driven storms.

[3]

The AMPTE satellite revealed the presence of molecular NO^+ and O_2^+ ions at L ~ 6.5–7 in the equatorial magnetosphere with energies of approximately 100 keV/q during storms, while there were no molecular ion events during geomagnetically quiet times (Klecker et al., 1986). The AMPTE observations also showed that molecular ions were detected a few to 16 h after sudden storm commencement (SSC). These molecular ions contributed ~0.5% of the total energy of 32 keV/cm^{-3} in the energy range of 20–230 keV/q (Klecker et al., 1986). The presence of these energetic molecular ions suggests that their efficient heating during transport from the ionosphere to the magnetosphere is influenced by mass-dependent energization mechanisms or the density profile of the thermosphere during storms. Model calculations (Sojka and Schunk, 1984) have shown that the densities of molecular ions above ~ 300 km increase by several orders of magnitude during the main phase of a magnetic storm. Data observed by Geotail/STICS in the magnetotail over 20 years (1995-2015) showed that the molecular ion count rates of magnetospheric molecular ions have a strong response to geomagnetic activity. Moreover, molecular ions and atomic N^+ and O^+ ions react differently to the solar F10.7 flux (Christon et al., 2020).

[4]

Lin and Ilie (2022) reviewed the past observations of magnetospheric molecular ions and concluded that the probability of observing molecular ions in the magnetosphere during quiet periods was nearly negligible. Recently, the Arase satellite has observed molecular ions more frequently in the inner magnetosphere. Using Arase satellite data, Seki et al. (2019) reported that molecular ions are frequently observed at L=2.5-6.6 during storms. The frequent appearance of molecular ions in the inner magnetosphere suggests a higher occurrence of molecular ion outflows during storm periods than previously estimated, as earlier studies presumed that molecular ions were only detectable during severe storms (Dst ≤ -100 nT). These results suggest that magnetic storms are not always necessary for molecular ion enhancement, and systematic observations of molecular ions are necessary to reveal the occurrence of molecular ions in the inner magnetosphere. In this study, we analyze systematic molecular ion observation data obtained by the Arase satellite since April, 2017 during the late declining phase of the solar cycle 24 and early rising phase of the solar cycle 25. This period covers quiet geomagnetic conditions, as well as several severe magnetic storms. Using Arase time-of-flight (TOF) data, we investigated long-term variations in molecular ions and their dependence on geomagnetic activity and solar wind parameters.

2 Analysis of the Arase TOF data

[5]

In this study, we used data from the LEPi instrument (Asamura et al., 2018) onboard the Arase satellite (Miyoshi et al., 2018), which covers energies from 0.01 to 25 keV/q. LEPi uses TOF method to measure the flight time of incoming ions inside a sensor to differentiate ion species. LEPi has two observation modes: normal and TOF. In the normal mode, LEPi provides ion fluxes as a function of energy, incoming direction, and ion species estimated by the measured particle TOF. In the TOF mode, the ion fluxes are provided as a function of the measured

particle TOF rather than the estimated species, allowing minor ions to be observed. The TOF mode is typically used during the outbound pass of every fourth orbit.

[6]

Figure 1(a) and (b)show energy spectra of H^+ and O^+ count rates observed in the TOF mode from 15:16 to 19:50 UT on May 28, 2017. During this time period, the satellite traversed from L=2.5 to 6.0 on the morning side under the early phase of recovery following a storm on May 28. Enhancements in the H^+ and O^+ ion count rates associated with storms are particularly noticeable after 16:30. **Figure 1(c)** shows the accumulated counts as a function of TOF (measured flight time) and energy during this time period. The TOF depends on both the mass and energy of each ion species. Although LEPi detected multiple ion species in the inner magnetosphere, there are fewer counts at low energies, and the peaks are closely spaced at higher energies, making it more difficult to distinguish the individual peaks. Therefore, we focused on the data obtained at 19. 2 keV/q, since significant counts and clear peaks depending on ion species are obtained. **Figure 1(d)** shows the TOF profile at an energy of 19.2 keV/q (black lines). A tail of the ion peaks toward longer TOF in **Figure 1(d)** is due to energy loss and angular straggling of incoming ions passing through the ultra-thin carbon foil installed in the instrument. The tail of O^+ TOF profile overlaps to the TOF profile of molecular ions, where the accumulated count of molecular ions (highlighted in purple) is approximately two orders of magnitude smaller than that of O^+ (highlighted in yellow). It is necessary to remove this O^+ tail influence to accurately determine the molecular ion count.

[7]

To estimate the actual molecular ion counts for LEPi TOF, it is important to estimate the background counts, including the O^+ ion counts and ambient noise. Several methods have been developed for deriving ion counts from TOF observations of the satellites. Seki et al. (2019) applied Gaussian function fitting to derive molecular ions for the Arase/MEPi observations. Mouikis et al. (2014) applied a subtraction method to estimate the background noise for the Cluster/CODIF observations. Since the molecular ion counts detected by LEPi were too small to estimate with fitting, we constructed “a reference profile” to model the O^+ TOF profile, as shown by the red line in **Figure 1(d)**. First, for each TOF spectrum, count averaged over 312 to 390 ns, where there are no significant TOF profiles of major ion species, was subtracted from all the TOF bins, since the noise source such as penetrating radiations appears as constant counts over the TOF spectrum. Then, to define the reference profile, we selected the TOF spectrum on March 15, 2023 as the reference in which the O^+ TOF profile was well identified without any significant counts of molecular ions. To obtain the smooth reference profile, we performed a quadratic least squares fit to the reference TOF profile ranging from 60 to 86 ns which covers the major part of the TOF spectrum of molecular ions. Then the reference profile was normalized to the O^+ peak count of each observation. Molecular ion count was obtained by subtracting the reference profile from the observed TOF spectrum and summed over the TOF range of molecular ions (purple). In case of **Figure 1(d)**, the counts of H^+ and O^+ are 4.5×10^6 and 3.9×10^6 that are estimated from the same fitting method as Funsten et al. (2013), while the count of molecular ions estimated from this method is 8.2×10^3, which is small compared to those for H^+ and O^+. After visual

inspection of all the Arase TOF data for 6.5 years from April 2017 to December 2023, the count data without a significant peak for molecular ions were eliminated from the further analysis in this study.

3 Results

[8]

Figure 2 shows molecular ion counts observed in two distinct events. The panels show the molecular ion counts, *L*-value where Arase was located, IMF Bz, solar wind speed, solar wind dynamic pressure, SYM-H index, and SML index on July 19, 2019 (**Figure 2(a)**) and March 14, 2022 (**Figure 2(b)**). Molecular ion counts were estimated by accumulating data over a 10-minute period. Blue shaded areas indicate the time intervals of the TOF mode measurements using the LEP-i instrument. As shown in Figure 2, these events are driven by CIR and CME (Miyoshi and Kataoka, 2005).

[9]

The first event was caused by a CIR and subsequent coronal hole stream. The amplitude of the minimum SYM-H index was -42 nT. Molecular ions were detected during the recovery phase, and the maximum count was 947 at L=5.28 after the sudden commencement (SC) caused by an enhancement in the solar wind dynamic pressure of up to 19.1 nPa. It is worth noting that molecular ions were not found in the TOF observations at 3:28 – 7:45 on July 9, immediately after the SC. This implies that ion transport from the ionosphere to the magnetosphere requires a finite time. This observation shows that molecular ions associated with the solar wind dynamic pressure enhancement can exist in the inner magnetosphere without severe magnetic storms.

[10]

The second event was driven by a CME. Sheath and magnetic clouds were observed, and the minimum SYM-H index was – 114 nT. The maximum count was approximately 1344 at L= 4.18. The SC was observed in association with the enhancement of solar wind dynamic pressure up to 17.7 nPa. Molecular ions were observed during the storm recovery phase. While the storm amplitude and solar wind drivers were different from those of the first event, the SC caused by solar wind dynamic pressure enhancement was commonly observed before the increase in the

molecular ion count in the inner magnetosphere. This is consistent with previous observations (Klecker et al., 1986) that molecular ions are observed after SSC.

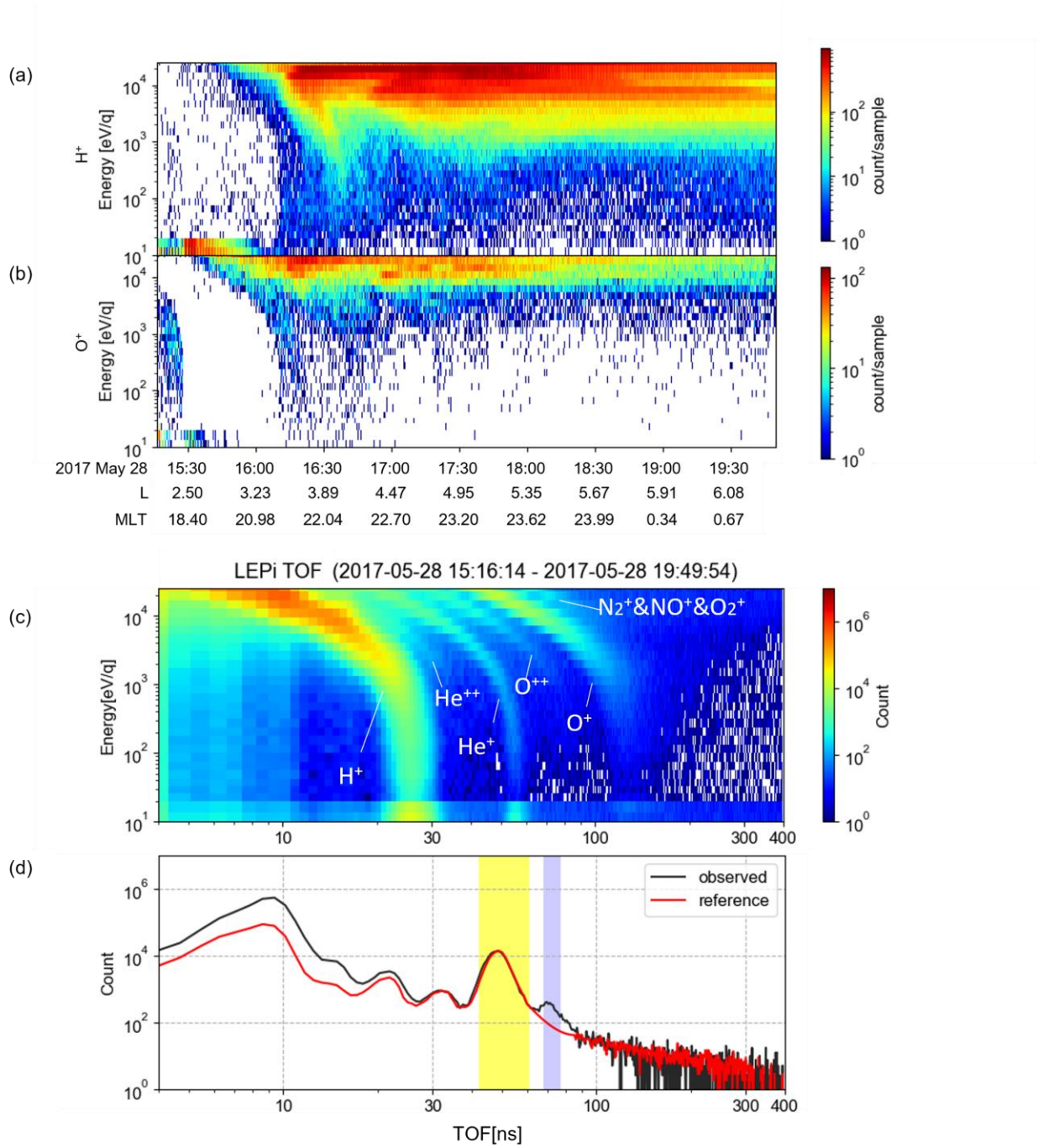

Figure 1. Time-energy diagram of **(a)** H^+ and **(b)** O^+ observed at 15:16-19:50 UT on May 28, 2017 for consideration of time variation of count rate change over pass. **(c)** TOF-energy diagram observed at the same time interval. The color indicates the counts of ions. **(d)** TOF spectrum on May 28, 2017 at 19.2 keV/q. Observed data (black line), reference profile (red line), TOF range

of O^+ (yellow shaded), and TOF range of molecular ions (purple shaded); **(c)** and **(d)** shows the data summed within 1 outbound pass.

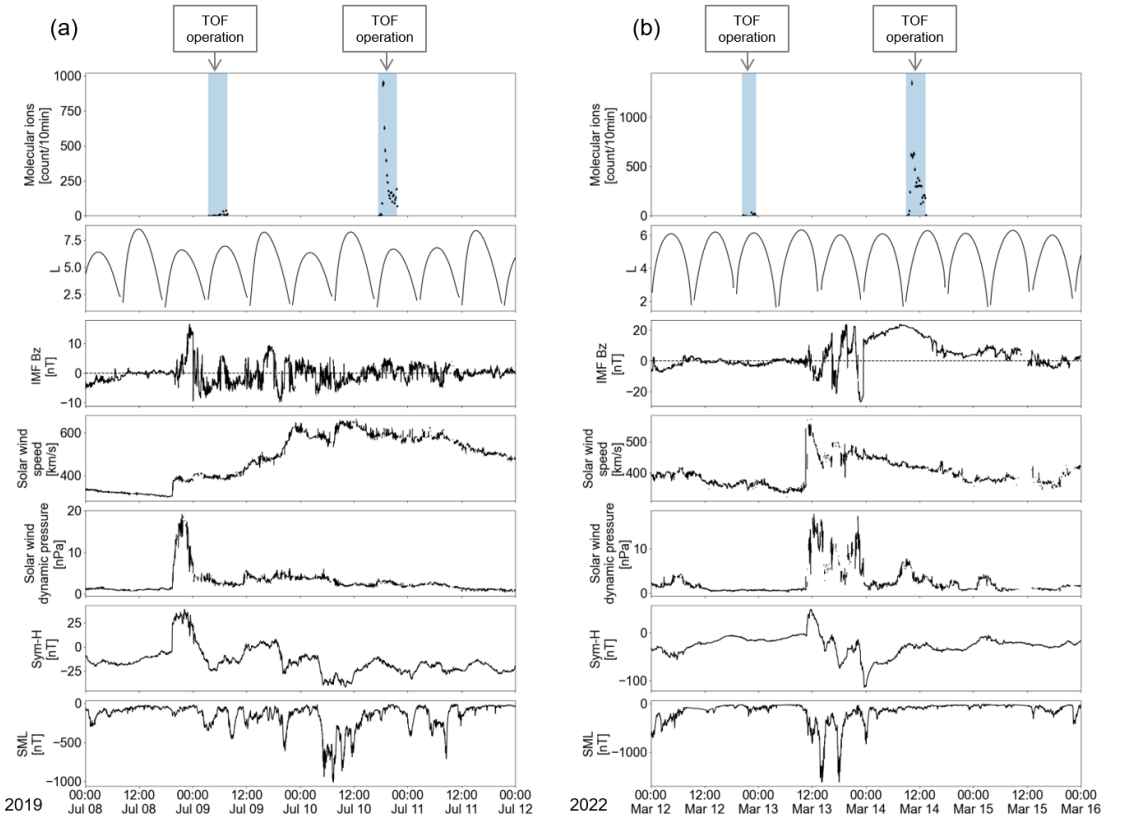

Figure 2

Figure 2. LEPi detected molecular ions events on **(a)** July 10, 2019, **(b)** March 14, 2022. From top to bottom, molecular ion count, *L*-value of the Arase satellite, IMF Bz, solar wind velocity, solar wind dynamic pressure, SYM-H, and SML index respectively. The blue shaded areas in the top panels show the time intervals of TOF mode operation.

[11]

Next, we show the parameter dependence of the molecular ion counts. We found 14 clear molecular ion events from Arase observations over 6.5 years. **Table S1** shows the 14 observed events. 13 of the 14 events were associated with CIR or CME. As can be seen from the table, on April 4 and 5, 2017 and May 28 and 29, 2017 molecular ions were observed in two consecutive observation passes. For the correlation analysis hereafter, the molecular ion counts on April 4 and May 28 will be used as representatives for these events. **Figures 3 (a)**, **(b)**, and **(c)** show the correlation between the molecular ion count and solar wind dynamic pressure, SYM-H index,

and SML index for these events. The parameter used for this correlation study was the maximum absolute value of the parameter within two days before molecular ion detection. The molecular ion count increased with the solar wind dynamic pressure, and increased twofold when the solar wind dynamic pressure increased by a factor of 1.5. The correlation coefficient between the molecular ion count and solar wind dynamic pressure was 0.68. In all events, solar wind dynamic pressure enhancement occurred before the observation of the molecular ions. The correlation with the SYM-H index was also significant; the molecular ion count increased at the same rate as that for the SYM-H index; the correlation coefficient was -0.75. It is important to note that the minimum SYM-H of the six events is higher (less negative) than -50 nT, indicating that molecular ions can exist in the inner magnetosphere during non-storm times if there is a solar wind dynamic pressure enhancement. The molecular ion counts showed a good correlation with the SML index, with a correlation coefficient of -0.70. Note that the SML index has not been available for the September 18, 2023 event, the correlation coefficient is estimated from other 13 events. It was found that there is a relationship between magnetospheric molecular ion counts

and the intensity of substorms. We also investigated the correlations between the solar wind velocity; however, the correlation coefficient was lower than 0.5.

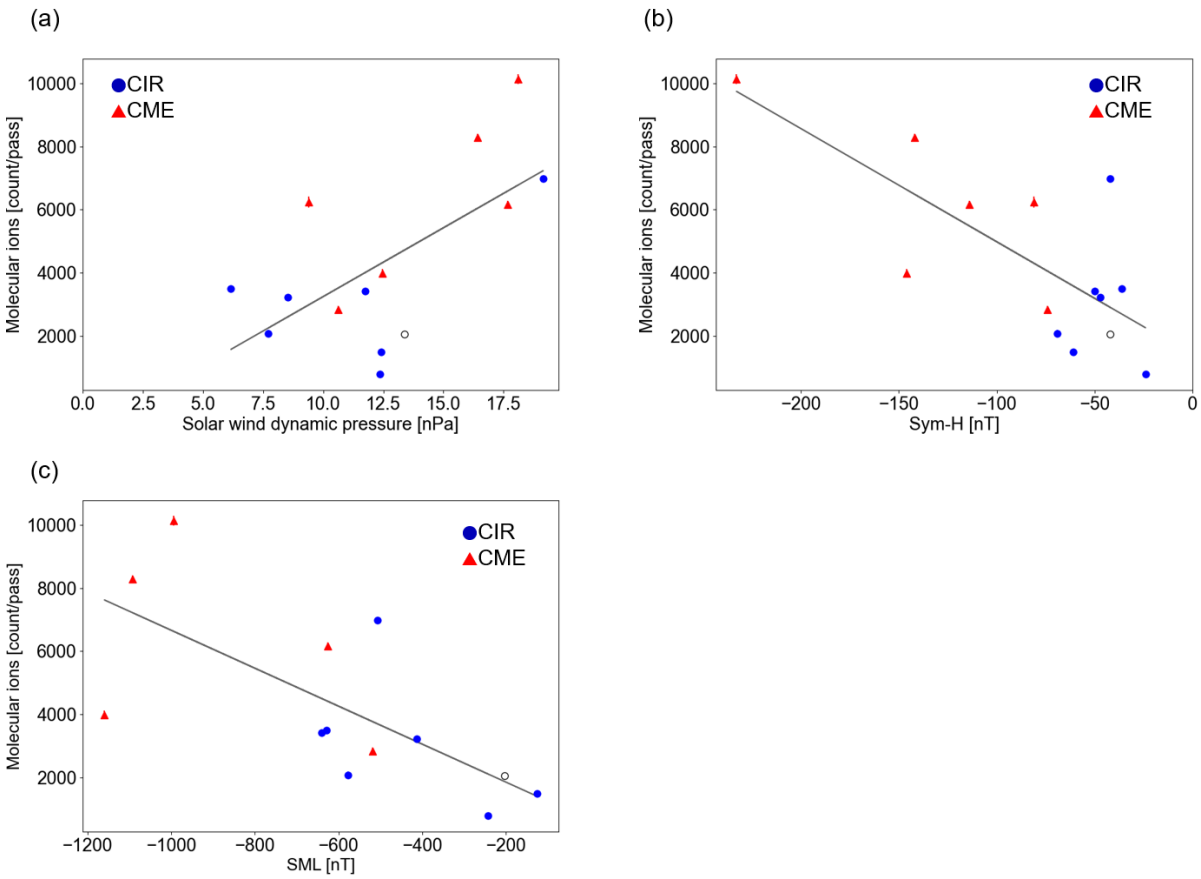

Figure 3. Relationship between the molecular ion counts and **(a)** solar wind dynamic pressure, **(b)** SYM-H index, and **(c)** SML index. Blue dots are related to CIR and red triangles are related to CME.

[12]

To obtain sufficient counts of molecular ions, we integrated the TOF profile data for six months. When a clear peak for the molecular ions was observed, we derived the molecular ion counts using the same method as that in the previous analysis. The peak of the molecular ions in the TOF profile was not clear after the second half of 2021, probably owing to enhancements in

oxygen ions. The red dots in **Figure 4(b)** after the end of 2021 represent the cases in which there were no significant molecular ion peaks in the TOF profiles (red circles).

[13]

Figure 4 shows the time variations of the molecular ion counts, oxygen ion counts, and ratio of molecular ions to oxygen ion counts. **Figure 4(a)** shows the long-term variations in the oxygen ion counts. The variation in oxygen ion counts seems to correlate with solar activity. When Arase observations began in 2017, counts were on the order of 5×10^4, falling to approximately one-fifth of that by the first half of 2020. Thereafter, as the solar activity increased, the counts increased to 2×10^6 in early 2023. **Figure 4(b)** shows the long-term variations in molecular ion counts (N_2^+, NO^+, and O_2^+). In contrast to the oxygen ions, the molecular ions showed count enhancements in early 2017, late 2019, and early 2021, with the variability unrelated to the solar activity. Note that the data shown in red beyond the latter half of 2021 indicates that the molecular ion peak was not clearly observed.

[14]

Figure 4(c) shows the ratio of the molecular ion count to the oxygen ion count. The ratio peaks during the solar minimum, in contrast to the oxygen profile. If the same process contributes to the escape of both molecular and oxygen ions, they should exhibit the same systematic variations. These results suggest that different processes are responsible for the outflow of these ionic species. Note that the molecular ion peak in the TOF spectrum disappears when the ratio

drops below ~1.5×10^{-3}, and thus, the upper limit is below the ratio measured during other time periods shown in black circles.

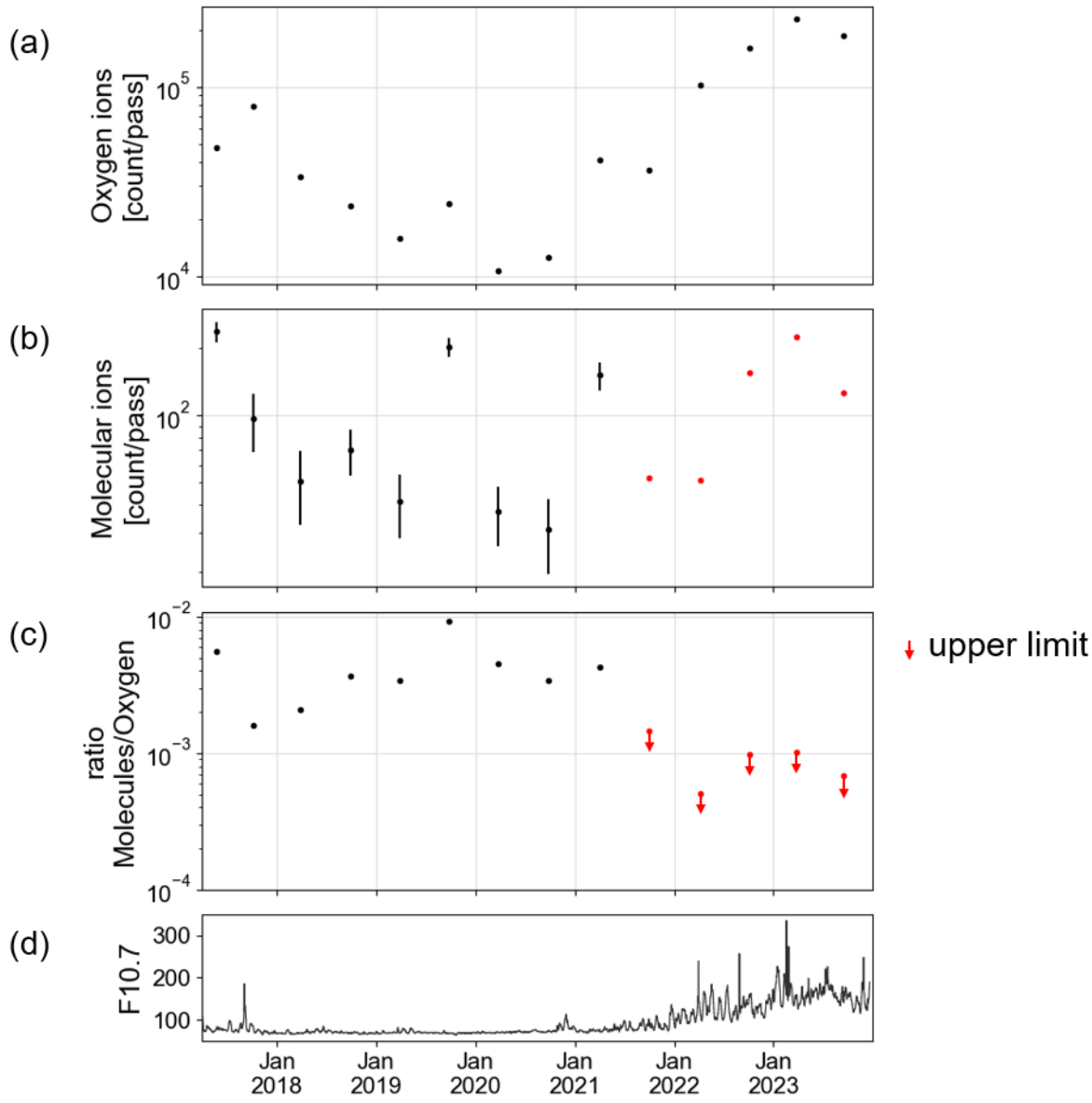

Figure 4 (a) Oxygen ion count, **(b)** molecular ion count, **(c)** ratio of molecular ion count to oxygen ion count with the data summed and averaged over half a year. **(d)** The bottom panel shows the F10.7 flux. The red circles in **(b)** correspond to the cases in which there were no

significant molecular ion peaks in the TOF profiles. The downward arrow in **(c)** indicates the upper limit.

4 Summary and Discussions

[15]

In this study, we investigated the molecular ions in the inner magnetosphere observed by the Arase satellite, which is the first observation of long-term variations in molecular ions in the inner magnetosphere. To quantitatively investigate the molecular ions, we developed a method to estimate the molecular ion counts from the TOF data. This method effectively eliminated the influence of the O^+ TOF profile on the molecular ion TOF range and yielded a reliable dataset. The estimated molecular ion counts showed good correlations with the solar wind dynamic pressure, SYM-H index, and SML index.

[16]

Previous studies have suggested that molecular ions in the inner magnetosphere are observed during large geomagnetic storms (Craven et al., 1985, Klecker et al., 1986), because a strong energy input is necessary for molecular ions to escape from the upper atmosphere. Seki et al. (2019) showed that energetic molecular ions are observed during small magnetic storms (Dst ~-20 nT) from the Arase observations in 2017. As shown in **Figure 3(b)**, molecular ions can be observed even during non-storm times (SYM-H > -30 nT) under significant enhancement of solar wind dynamic pressure.

[17]

Schunk et al. (1975) show that owing to the rapid increase of the reaction $O^+ + N_2 \rightarrow NO^+ + N$ with ion energy, high-latitude electric fields deplete O^+ in favor of NO^+ after the increase of the scale height of N_2. For large electric fields (~200 mV m^{-1}), NO^+ completely dominates the ion composition up to at least 600-km altitudes. This reaction leads to a reduction in O^+ and enhancement in NO^+ during periods of intense convection velocity. Wilson and Craven (1999) demonstrated that the outflow of molecular ions necessitates specific conditions based on the DE-1 observations, one of which is the presence of strong convection electric fields in the ionosphere.

[18]

It should be noted that all events in **Figure 3(a)** are associated with a solar wind dynamic pressure enhancement of more than 5 nPa during both storm and non-storm intervals. As shown in **Figure 2**, SSCs caused by solar wind dynamic pressure enhancement were detected in ~85% of the molecular ion events. The results suggest that the energy input associated with the solar wind dynamic pressure is essential for the outflow of molecular ions from the upper atmosphere

to the inner magnetosphere, as suggested by AMPTE observations（Klecker et al., 1986). Gillie et al. (2012) indicated that ionospheric convection is enhanced in association with SSC. The results of this study suggest that an increase in the solar wind dynamic pressure leading to SSC or SC events results in an increase in the convection electric field, which facilitates the production and outflow of molecular ions into the magnetosphere. Enhancements in convection electric fields are also observed during storm times; therefore, it is natural to find a correlation between the SYM-H index and molecular ion counts, as shown in **Figure 3(b)**.

[20]

Figure 4 shows the long-term variations in the molecular and oxygen ions in the inner magnetosphere, where no systematic variations in the molecular ion counts are observed. The molecular ion to oxygen ratio is the inverse of the oxygen count profile, and a potential scenario to explain the long-term variations is as follows: during periods of solar minimum when the scale height of O^+ is reduced, the reaction responsible for converting O^+ to NO^+ in the presence of strong convection (Schunk et al., 1975) has a significant impact on the resulting composition of the outflow, as evidenced by Arase observations that indicate a noticeable increase in molecular ions. By contrast, during the solar maximum, when the scale height of O^+ is higher, the outflow of O^+ occurs more readily. Since the outflow of oxygen ions far exceeds that of molecular ions, it is likely that the molecular ions/O^+ ratio remains too low to be detected even when the flux of the molecular ion outflow increases. This result is consistent with the observations from Geotail, as reported by Christon et al. (2020), indicating that atomic and molecular ions demonstrate different responses to F10.7.

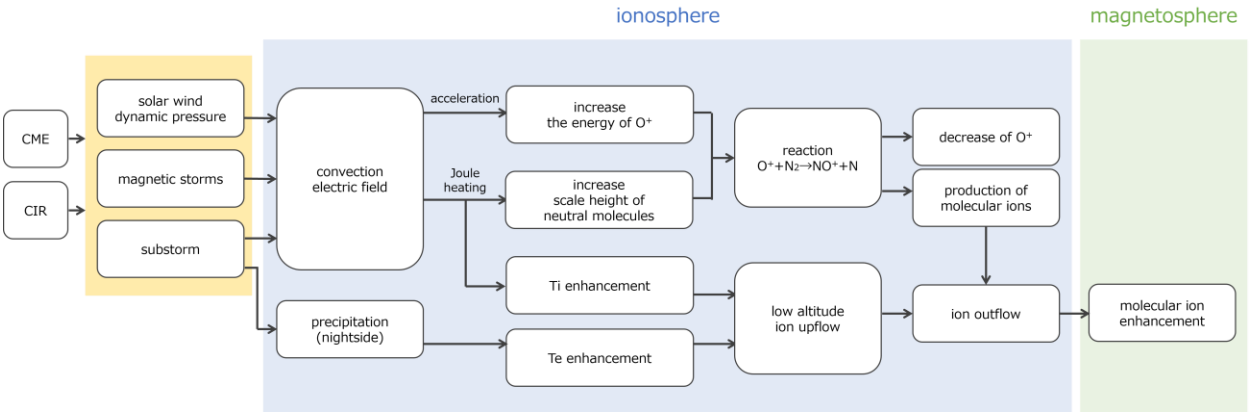

Figure 5 Schematic diagram for the possible process leading to molecular ion outflow.

[21]

Figure 5 shows a schematic diagram to summary the possible process based on these results. An increase in solar wind dynamic pressure leads to an increase in the convection electric field. The enhancement of the convection electric field influences the scale height of the neutral molecules via the Joule heating and increases the energy of the oxygen ions. These processes lead to the

production of molecular ions by enhancing the reaction between oxygen ions and neutral molecules. This reaction causes a decrease in O^+ and an increase in NO^+ (Schunk et al., 1975), which is consistent with the results in **Figure 4**. As demonstrated by Takada et al.(2021), the ion frictional heating resulting from the convection electric field triggers ion upflow in the ionosphere. Taking this into account, it is conceivable that solar wind dynamic pressure enhancement leads to ion upflow, which is comparatively rich in molecular ions. The observed correlations between SYM-H and magnetospheric molecular ion counts (**Figure 3(b)**), as well as the solar wind dynamic pressure and magnetospheric molecular ion counts (**Figure 3(a)**), are consistent with this mechanism. It should be noted that the particle precipitation on the nightside also causes the low-altitude ion upflow during CIR-driven magnetic storms and small CME-driven storms (Takada, 2023). As shown in **Table S1**, our result shows that over 90% of the events were observed associated with arrivals of CIR or CME in which an increase of precipitation is expected. Therefore, it is suggested that particle precipitation in addition to the enhancement of the convection electric field may also contributes to the enhancement of molecular ions in the magnetosphere.

[22]

Considering the molecular ion upflow mechanisms, enhancement of convection electric fields is essential. Solar wind dynamic pressure enhancement, magnetic storms, and substorms contribute to the enhancement of the convection electric fields that drive the molecular ion upflow. As shown in this study, molecular ions can exist in the inner magnetosphere associated with a pressure enhancement even during non-storm periods. The oxygen and the molecular ions scale heights depend on the solar cycle. Since the Arase observations in this study did not cover the solar maximum, further observations of molecular ions in the inner magnetosphere are important to clarify the outflow mechanism of molecular ions.

Acknowledgments

This study is supported by JSPS grant (20H0159, 21H04526, 22K21345, 23H01229).

Data Availability Statement

The data for this study is archived in the ERG Science Center (ERG-SC) operated by ISAS/JAXA and ISEE/Nagoya University (https://ergsc.isee.nagoya-u.ac.jp/index.shtml.en; Miyoshi, Hori, et al., 2018). The present study used the Arase/LEPi data L2-v03 (Asamura, Miyoshi and Shinohara, 2018, 10.34515/DATA.ERG-05001) and the Arase orbital data L2-v03 (Miyoshi, Shinohara, and Jun, 2018, 10.34515/DATA.ERG-12000) . The Sym-H index (WDC Kyoto, 2022, 10.14989/267216) used in this paper/presentation was provided by the WDC for Geomagnetism, Kyoto (http://wdc.kugi.kyoto-u.ac.jp/wdc/Sec3.html). The solar wind and IMF data were obtained from NASA/GSFC's OMNI data set through the OMNIWeb (https://omniweb.sci.gsfc.nasa.gov). The SML index is provided from SuperMAG (http://supermag.jhuapl.edu/indices).

References

Asamura, K., Y. Kazama, S. Yokota, et al.(2018), Low-energy particle experiments–ion mass analyzer (LEPi) onboard the ERG (Arase) satellite. *Earth Planets Space*, **70**, doi: 10.1186/s40623-018-0846-0

Asamura, K., Y. Miyoshi, and I. Shinohara(2018), The LEPi instrument Level-2 omniflux data of Exploration of energization and Radiation in Geospace (ERG) Arase satellite, doi:10.34515/DATA.ERG-05001.

Craven, P. D., R. C. Olsen, C. R. Chappell, and L. Kakani (1985). Observations of Molecular Ions in the Earth's Magnetosphere. *J. Geophys. Res.*, **90**, 7599–7605. doi:10.1029/JA090iA08p07599

Christon, S. P., D. C. Hamilton , D. G. Mitchell, J. M. C. Plane, and S. R. Nylund (2020). Suprathermal magnetospheric atomic and molecular heavy ions at and near Earth, Jupiter, and

Saturn: Observations and identification. *J. Geophys. Res.*, **125**, e2019JA027271, doi:10.1029/2019JA027271

Funsten, H. O. et al. (2013), Helium, Oxygen, Proton and Electron (HOPE) mass spectrometer for the radiation belt storm probe mission, *Space Sci. Rev.*, **179**, 423-484, doi:10.1007/s11214-013-9968-7.

Gillies, D. M., J.-P. St.-Maurice, K. A. McWilliams, and S. Milan (2012), Global-scale observations of ionospheric convection variation in response to sudden increases in the solar wind dynamic pressure, *J. Geophys. Res.*, **117**, A04209, doi:10.1029/2011JA017255.

Glocer, A., N. Kitamura, G. Toth, and T. Gombosi (2012). Modeling solar zenith angle effects on the polar wind. *J. Geophys. Res*. **117**, A04318. doi:10.1029/2011JA017136

Ilie, R., M. W. Liemohn, G. Toth, N. Ganushkina, and L. K. S. Daldorff (2015). Assessing the role of oxygen on ring current formation and evolution through numerical experiments. *J. Geophys. Res. Space Phys*. **120**, 4656–4668. doi:10.1002/2015JA021157.2015JA021157

Keika, K., L. M. Kistler, and P. C. Brandt (2013). Energization of O^+ ions in the Earth's inner magnetosphere and the effects on ring current buildup: A review of previous observations and possible mechanisms. *J. Geophys. Res.*, **118**, 4441–4464.、doi:10.1002/jgra.50371

Klecker, B., E. Möbius, D. Hovestadt, M. Scholer, G. Gloeckler, and F. M. Ipavich (1986). Discovery of energetic molecular ions ($NO^+$and O_2^+) in the storm time ring current. *Geophys. Res. Lett.* **13**, 632–635. doi:10.1029/GL013i007p00632

Lennartsson, O.W., H.L. Collin, W.K. Peterson, and E.G. Shelley, (2000) Polar/TIMAS statistical results on the outflow of molecular ions from earth at solar minimum, *Adv. Space Res.*, **25**, doi:10.1016/S0273-1177(99)00531-1.

Lin M-Y and R. Ilie (2022) A Review of Observations of Molecular Ions in the Earth's Magnetosphere Ionosphere System. *Front. Astron. Space Sci*. 8:745357. doi: 10.3389/fspas.2021.74535

Miyoshi, Y., I. Shinohara, T. Takashima et al.(2018), Geospace exploration project ERG. *Earth Planets Space*, **70**, 101, doi:10.1186/s40623-018-0862-0

Miyoshi, Y., and R. Kataoka (2005), Ring current ions and radiation belt electrons during geomagnetic storms driven by coronal mass ejections and corotating interaction regions, *Geophys. Res. Lett.* **32**, L21105, doi:10.1029/2005GL024590.

Miyoshi, Y., T. Hori et al., (2018), The ERG Science Center, *Earth, Planets Space*, **70**, doi:10.1186/s40623-018-0867-8.

Miyoshi, Y., I. Shinohara, and C.-W. Jun(2018), The Level-2 orbit data of Exploration of energization and Radiation in Geospace (ERG) Arase satellite, 10.34515/DATA.ERG-12000, 2018.

406 Seki, K., K. Keika, S. Kasahara, S. Yokota, T. Hori, K. Asamura, et al.(2019). Statistical
407 properties of molecular ions in the ring current observed by the Arase (ERG) satellite. *Geophys.*
408 *Res. Lett.*, **46**, 8643–8651. doi:10.1029/2019GL084163

409 Schunk, R. W., W. J. Raitt, and P. M. Banks (1975), Effect of electric fields on the daytime high-
410 latitude E and F regions, *J. Geophys. Res.*, **80**(22), 3121–3130, doi:10.1029/JA080i022p03121.

411 Takada, M., K. Seki, Y. Ogawa, K. Keika, S. Kasahara, S. Yokota, et al. (2021). Low-altitude
412 ion upflow observed by EISCAT and its effects on supply of molecular ions in the ring current
413 detected by Arase (ERG). *J. Geophys. Res.*, **126**, e2020JA028951. doi:10.1029/2020JA028951

414 Takada, M.(2023), Study of ion upflows in the low-altitude ionosphere and their effects on
415 supply of terrestrial heavy ions to the magnetosphere, doctorate in Science, University of Tokyo,
416 UTokyo Repository: http://hdl.handle.net/2261/0002008367

417 World Data Center for Geomagnetism, Kyoto, S. Imajo, A. Matsuoka, H. Toh, and T. Iyemori
418 (2022), Mid-latitude Geomagnetic Indices ASY and SYM (ASY/SYM Indices),
419 doi:10.14989/267216.

420 Wilson, G. R., and P. Craven (1999), Molecular ion upflow in the cleft ion fountain, *J. Geophys.*
421 *Res.*, **104**(A3), 4437–4446, doi:10.1029/1998JA900070.

422 Yau, A. W., T. Abe, and W. K. Peterson (2007). The Polar Wind: Recent Observations. *J. Atmos.*
423 *Solar-Terr. Phys.*, **69**, 1936–1983. doi:10.1016/j.jastp.2007.08.010